

MULTIPLICITY DISTRIBUTION OF SECONDARY HADRONS AT LHC ENERGY AND TOTAL CROSS SECTIONS OF HADRON-HADRON INTERACTIONS

V.A. Abramovsky[†], N.V. Radchenko[‡]

Novgorod State University

[†] *E-mail: Victor.Abramovsky@nonsu.ru*

[‡] *E-mail: nvrad@mail.ru*

Abstract

The multiple production processes of secondary hadrons in proton-antiproton scattering are divided into three types. The first type is a shower of secondary hadrons produced from gluon string decay, the second type is a shower of secondary hadrons produced from two quark strings decay and the third is a shower produced from three quark strings decay. At the same time there are only two types for proton-proton scattering – shower from gluon string and shower from two quark strings. These showers do not correspond to pomeron showers originating from cuts of one, two, three, ... pomerons. Multiplicity distribution in gluon string is Gaussian, in two and three quark strings it is negative binomial. Gluon string weight in the multiplicity distribution is determined by the constant contribution to total cross sections, the quark strings weights – by the growing with energy contributions. The expected value of proton-proton scattering total cross section and the multiplicity distribution at energy 14 TeV are given.

1 Introduction

In most QCD models hadrons interaction is described by gluon ladders with large number of bars which is increasing with total energy \sqrt{s} [1]. These gluon ladders are associated with pomerons. For inelastic processes these amplitudes correspond to one or several parton cascades with large number of gluons. Mean multiplicity of secondary hadrons $\langle n(s) \rangle$ is proportional to mean number of partons $\langle \nu(s) \rangle$ with proportion coefficient which is of order one. Both these values are large and they sufficiently quickly grow with growth of total energy. It is very difficult in such models to adjust the large value of mean multiplicity with such observable values: 1) relations $\sigma_{tot}^{\pi^{\pm}p} / \sigma_{tot}^{pp} \simeq 2/3$ and $\sigma_{tot}^{K^{\pm}p} / \sigma_{tot}^{pp} < 2/3$ up to $\ln s \leq 7$; 2) limitation of secondary hadrons transverse momenta; 3) low value of Pomeranchuk trajectory slope.

In order to explain these contradictions there was proposed Low Constituents Number Model (LCNM) [2], [3] in which there are only valent quarks and low number of bremsstrahlung gluons in hadrons in initial state. The number of bremsstrahlung gluons grows slowly with growth of \sqrt{s} , and the interaction occurs as result of color exchange between quark and gluon. Secondary hadrons are produced when strings (tubes) of color electric field decay.

In this model we shall consider behavior of total cross sections and multiplicity distributions in processes of pp and $p\bar{p}$ interactions at high energies. These observables will be predicted for energy $\sqrt{s} = 14$ TeV.

2 Three types of hadrons production processes in proton-proton and proton-antiproton scattering

We describe the main processes of hadrons production in LCNM for pp and $p\bar{p}$ scattering by diagrams shown in Fig. 1 – Fig. 3.

In Fig. 1a $p\bar{p}$ interaction process is described when there are only valent quarks in initial state. Gluon exchange occurs between these colorless states, and components, which had obtained color charge, fly apart and form color field string. Since octet states fly apart it will be gluon string. Corresponding inelastic process of string decay is shown in Fig. 2. Dotted lines separate interaction in final state, which leads to gluons production (waved lines). Then these gluons form observable hadrons.

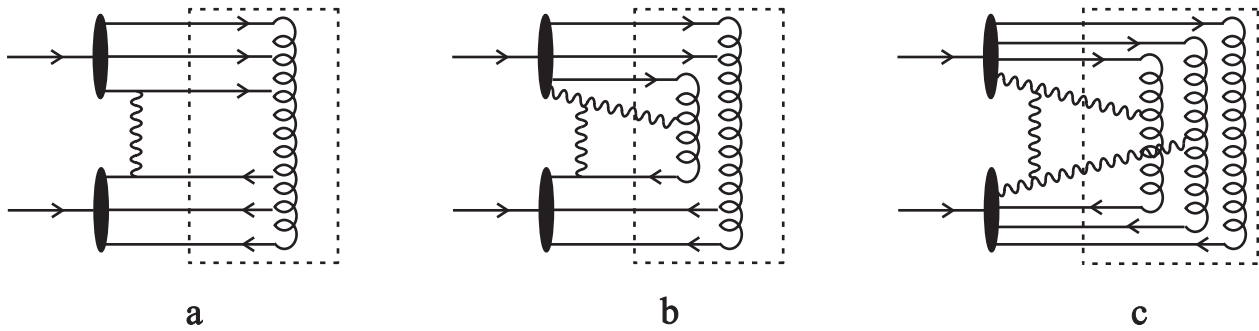


Figure 1: Three types of hadrons production processes in proton-antiproton scattering: a) hadrons production in gluon string; b) hadrons production in two quark strings; c) hadrons production in three quark strings. Interaction in final state, in which flying strings pass into hadrons, is separated by dotted lines. Interaction is achieved by gluon exchange (waved line) between different hadron components. Interacted gluons recharge quark strings in b and c variants.

This diagram gives the certain value of secondary hadrons multiplicity. Since there is a large number (practically infinite) of alike diagrams and since they all have approximately the same order, than the random value – secondary hadrons multiplicity – must obey normal distribution because of the probability theory central limit theorem. Thus we suppose that multiplicity distribution in the gluon string is Gaussian distribution.

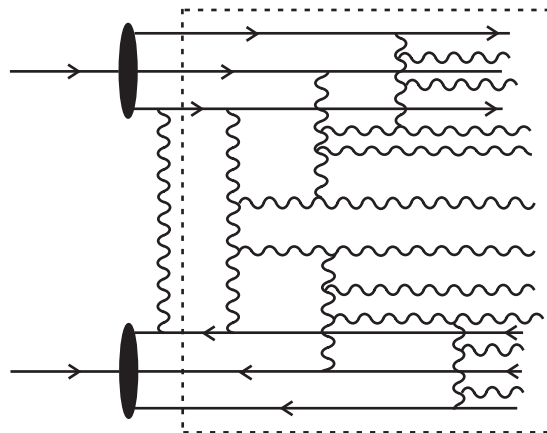


Figure 2: Diagram specifying gluon string decay from Fig. 1a.

We suppose that processes corresponding to diagrams with one additional bremsstrahlung

gluon (Fig. 1b) are inelastic processes with production of two divided quark strings. Generally speaking, transverse sizes of quark string must be in order of confinement radius, i. e. in order of hadron size. But since transverse momentum of additional bremsstrahlung gluon is rather large, approximately 1.5 – 2 GeV, than compton wave length of the gluon is small. This gluon must be absorbed at hadronization of one of the quark strings. Therefore corresponding quark strings must have transverse sizes comparable with gluon compton length.

Two bremsstrahlung gluons lead both to configuration with two quark strings and to configuration with three quark strings shown in Fig. 1c. Weights of configuration with two quark strings and three quark strings do not depend on energy.

Hadrons production processes in pp interaction differ from production processes in $p\bar{p}$ interaction (Fig. 3). There is no configuration with three quark strings in pp interaction since strings are produced between quark and diquark.

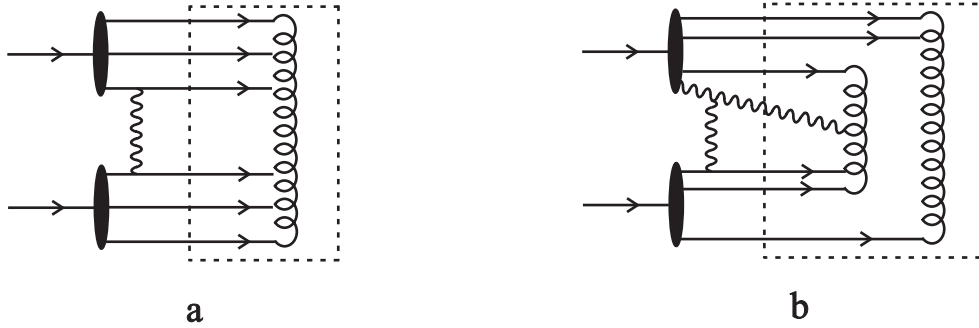


Figure 3: Two types of hadrons production processes in proton-proton scattering: a) hadrons production in gluon string; b) hadrons production in two quark strings.

We suppose that charged hadrons multiplicity distribution in quark string fulfills negative binomial distribution

$$P_n(k) = \frac{k(k+1)\dots(k+n-1)}{n!} \left(\frac{\langle n \rangle}{\langle n \rangle + k} \right)^n \left(\frac{k}{\langle n \rangle + k} \right)^k. \quad (1)$$

This distribution has two parameters: shape parameter k and mathematical expectation $\langle n \rangle$ – mean multiplicity. It is easy to show that convolution of two negative binomial distributions with the same $\langle n \rangle$ and k and convolution of three negative binomial distributions with the same $\langle n \rangle$ and k are also negative binomial distributions with $\langle n \rangle_2 = 2\langle n \rangle$, $k_2 = 2k$ and $\langle n \rangle_3 = 3\langle n \rangle$, $k_3 = 3k$.

$$\begin{aligned} P_n(k_2) &= \sum_{\substack{n_1, n_2 \\ n_1+n_2=n}} P_{n_1}(k) P_{n_2}(k) = \\ &= \frac{k_2(k_2+1)\dots(k_2+n-1)}{n!} \left(\frac{\langle n \rangle_2}{\langle n \rangle_2 + k_2} \right)^n \left(\frac{k_2}{\langle n \rangle_2 + k_2} \right)^{k_2}, \end{aligned} \quad (2)$$

$$\begin{aligned} P_n(k_3) &= \sum_{\substack{n_1, n_2, n_3 \\ n_1+n_2+n_3=n}} P_{n_1}(k) P_{n_2}(k) P_{n_3}(k) = \\ &= \frac{k_3(k_3+1)\dots(k_3+n-1)}{n!} \left(\frac{\langle n \rangle_3}{\langle n \rangle_3 + k_3} \right)^n \left(\frac{k_3}{\langle n \rangle_3 + k_3} \right)^{k_3}. \end{aligned} \quad (3)$$

3 Behavior of total cross sections of proton-proton and proton-antiproton scattering

Initial state components containing only valent quarks, containing valent quarks and one or two additional gluons, lead to different types of inelastic processes. It should be noted, that these inelastic processes differ from inelastic processes occurring both from cuts of pomeron and pomeron branchings. It also should be noted, that the third additional gluon in initial state gives negligible contribution. In accordance with this, total cross sections of pp and $p\bar{p}$ scattering can be written in form:

$$\sigma_{tot}^{p(\bar{p})p} = 63.52s^{0.358} \mp 35.43s^{0.56} + \sigma_0^{pp} + \sigma_1^{pp} \ln s + \sigma_2^{pp} (\ln s)^2, \quad (4)$$

where sign (-) stands for pp and (+) stands for $p\bar{p}$ interaction. The first two terms describe contributions from non vacuum reggeons exchange, the values and experimental data are taken from [4], σ_0^{pp} is contribution of gluon exchange between valent quarks, σ_1^{pp} is contribution of gluon exchange with components containing one additional gluon, σ_2^{pp} is contribution of gluon exchange with components containing two additional gluons. Parameters $\sigma_0^{pp} = 20.08 \pm 0.42$, $\sigma_1^{pp} = 1.14 \pm 0.13$, $\sigma_2^{pp} = 0.16 \pm 0.01$ were obtained from simultaneous fitting of pp and $p\bar{p}$ total cross sections. The result is shown in Fig. 4. Thus we can predict the value of total cross section σ_{tot}^{pp} for energy $\sqrt{s} = 14$ TeV $\sigma_{tot}^{pp} = 101.30 \pm 6.65$ mb.

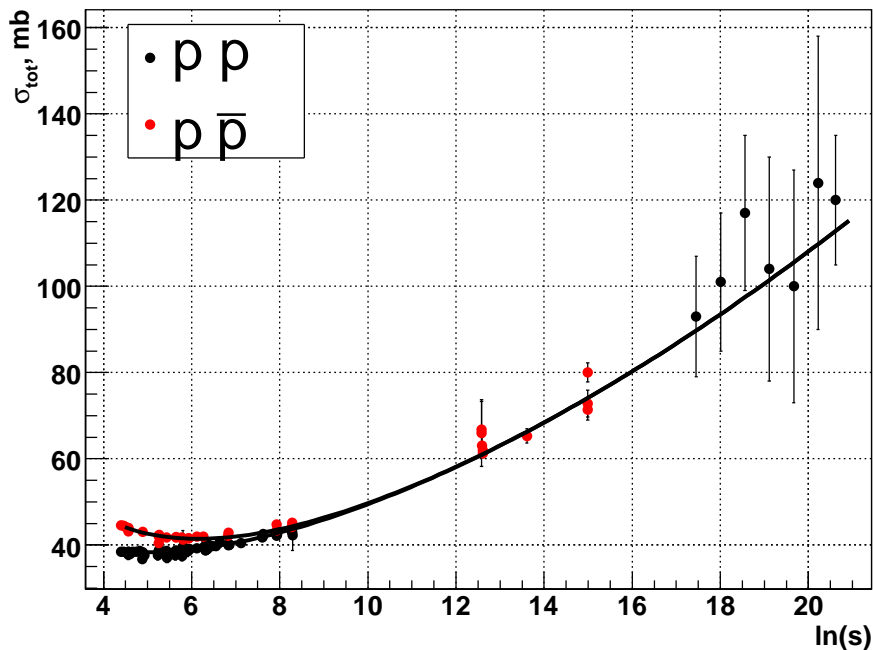


Figure 4: Total cross sections of proton-proton and proton-antiproton scattering.

We want to stress once more, that there is the possibility of only two additional bremsstrahlung gluons at energies up to LHC energy. With this assumption we fitted non single diffraction cross sections of pp and $p\bar{p}$ scattering [5], [6], [7], [8], [9].

$$\sigma_{nsd} = \sigma_{tot} - \sigma_{el} - \sigma_{sd}.$$

The contribution of non vacuum reggeons to elastic cross section σ_{el} and to single diffraction cross section σ_{sd} at energies higher than 44.5 GeV is low and we neglect it. Non vacuum

reggeons give contribution only to σ_{nsd} . We have subtracted this contribution from the experimental values of σ_{nsd} and obtained values of σ_{nsd}^{vac} – vacuum contributions to σ_{nsd} . Then we have fitted these values with formulae

$$\sigma_{nsd}^{vac} = \sigma_0^{nsd} (1 + \delta_1^{nsd} \ln s + \delta_2^{nsd} (\ln s)^2). \quad (5)$$

The parameter values are $\sigma_0^{nsd} = 14.50$ (fixed from physical considerations), $\delta_1^{nsd} = 0.0495 \pm 0.0105$, $\delta_2^{nsd} = 0.0073 \pm 0.0009$. The first term in (5) corresponds to gluon string contribution and defines area under normal distribution curve. The third term corresponds to two bremsstrahlung gluons contribution and, as it was explained above, defines contribution of three quark strings configuration $c_1 \sigma_0^{nsd} \delta_2^{nsd} (\ln s)^2$ and of two quark strings configuration $c_2 \sigma_0^{nsd} \delta_2^{nsd} (\ln s)^2$, at that, obviously, $c_1 + c_2 = 1$. The value of $c_1 \sigma_0^{nsd} \delta_2^{nsd} (\ln s)^2$ gives area under negative binomial distribution curve, corresponding to three quark strings configuration. Area under negative binomial distribution curve, corresponding to two quark strings configuration is given by expression $\sigma_0^{nsd} (\delta_1^{nsd} \ln s + c_2 \sigma_0^{nsd} \delta_2^{nsd} (\ln s)^2)$. The coefficients $c_1 = 0.23$ and $c_2 = 0.77$ were obtained from the fit and they do not depend on the energy of colliding particles.

4 Multiplicity distributions of charged hadrons of proton-proton and proton-antiproton scattering

We have fitted data on charged multiplicity distributions for non single diffraction processes in proton-antiproton scattering from experiments UA5 [6], [10] and E735 [11]. We suppose that multiplicity distribution is formed from the normal distribution for events with gluon string and two negative binomial distributions for events with two and three quark strings. We also suppose that parameters for every quark string both in configuration with two quark strings and in configuration with three quark strings are the same.

We have also fitted data on charged multiplicity distributions for non single diffraction processes in proton-proton scattering for energies $\sqrt{s} = 44.5$, $\sqrt{s} = 52.6$, $\sqrt{s} = 62.2$ GeV [9]. The results of fitting are shown in Fig. 5 – Fig. 24.

From these fits we have obtained parameters of normal distribution for gluon string $\langle n \rangle_g$ and σ and parameters of negative binomial distribution for quark string k and $\langle n \rangle_q$ for energy range from $\sqrt{s} = 44.5$ to $\sqrt{s} = 1800$ GeV. Then we have obtained the energy dependence of quark and gluon strings parameters and thus we obtained the values of parameters at energy $\sqrt{s} = 14$ TeV. The multiplicity distribution for LHC is shown in Fig. 25, 26. We can also calculate the value of mean charged multiplicity for LHC, it is $\langle n \rangle = 71.57 \pm 4.37$.

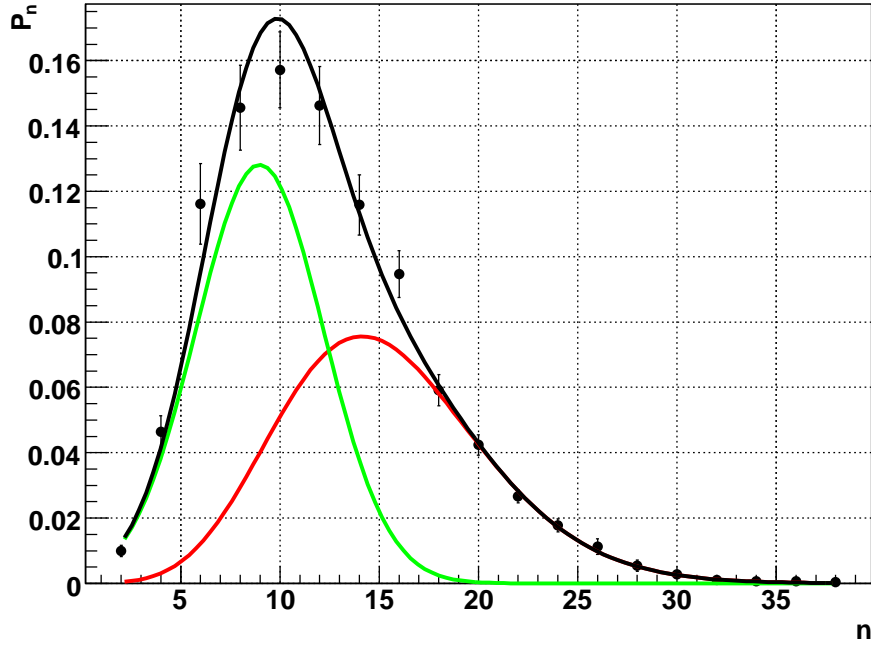


Figure 5: Charged multiplicity distribution for proton-proton scattering, $\sqrt{s} = 44.5$ GeV [9]. Red line – negative binomial distribution for two quark strings, green line – Gaussian distribution for gluon string, black line is sum of these distributions, $\chi^2/ndf = 13/14$.

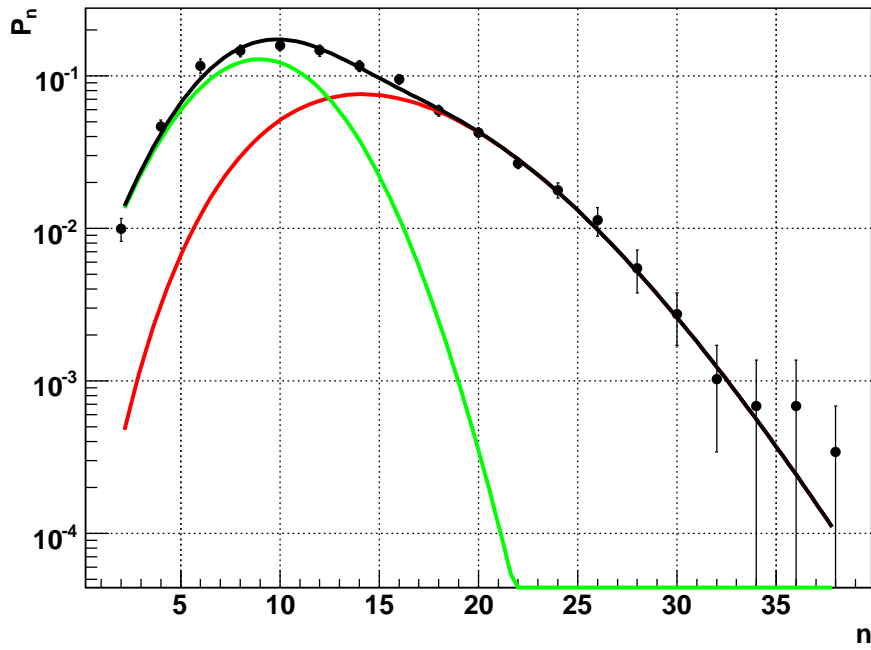


Figure 6: The same as for Fig. 5, logarithmic scale.

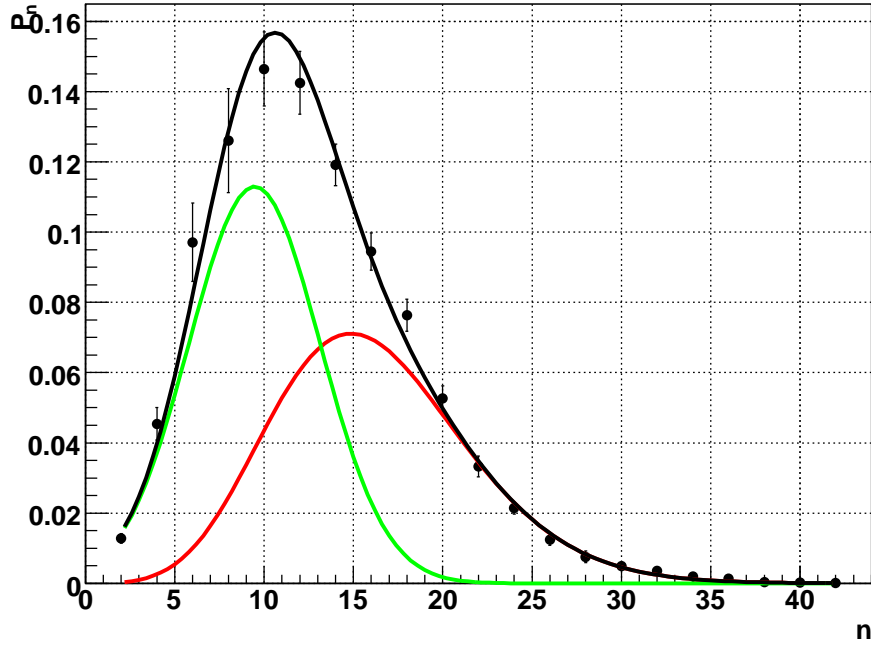


Figure 7: Charged multiplicity distribution for proton-proton scattering, $\sqrt{s} = 52.6$ GeV [9]. Red line – negative binomial distribution for two quark strings, green line – Gaussian distribution for gluon string, black line is sum of these distributions, $\chi^2/ndf = 17/16$.

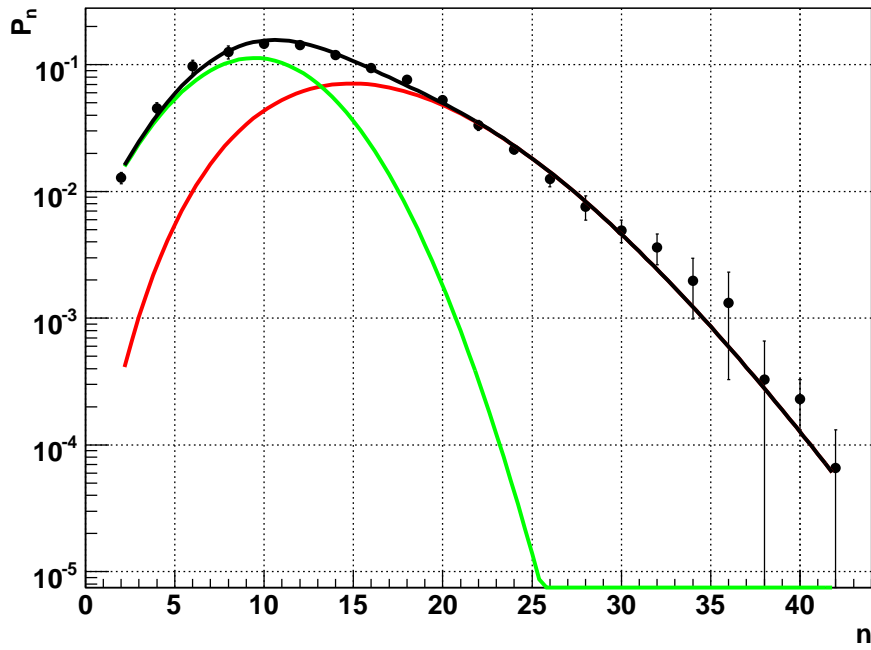


Figure 8: The same as for Fig. 7, logarithmic scale.

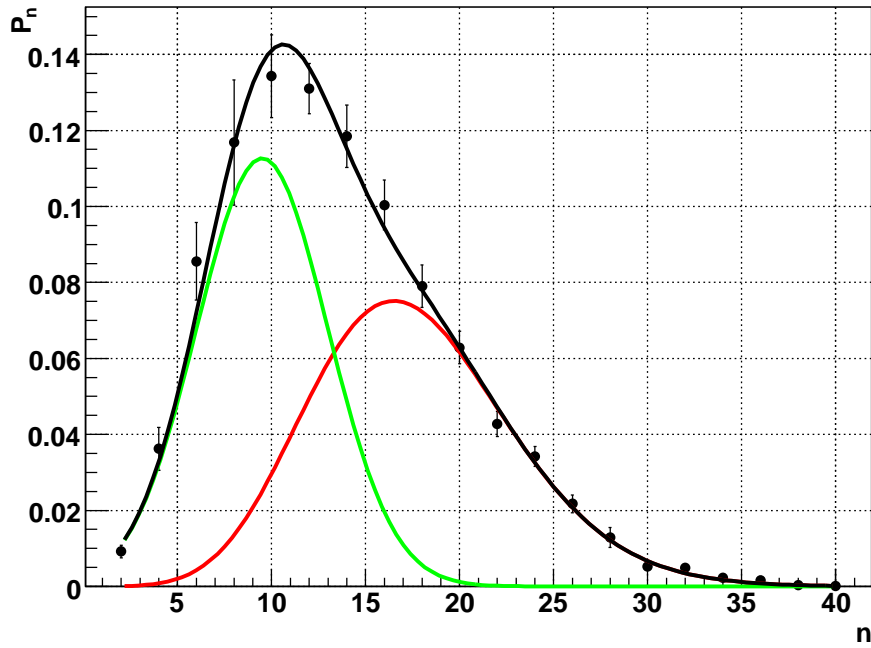


Figure 9: Charged multiplicity distribution for proton-proton scattering, $\sqrt{s} = 62.2$ GeV [9]. Red line – negative binomial distribution for two quark strings, green line – Gaussian distribution for gluon string, black line is sum of these distributions, $\chi^2/ndf = 13/15$.

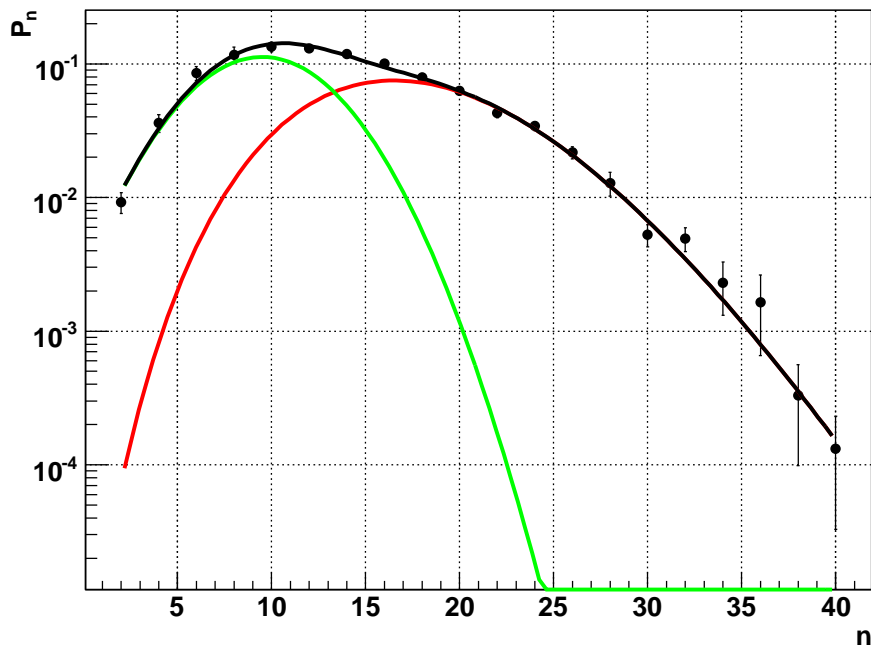


Figure 10: The same as for Fig. 9, logarithmic scale.

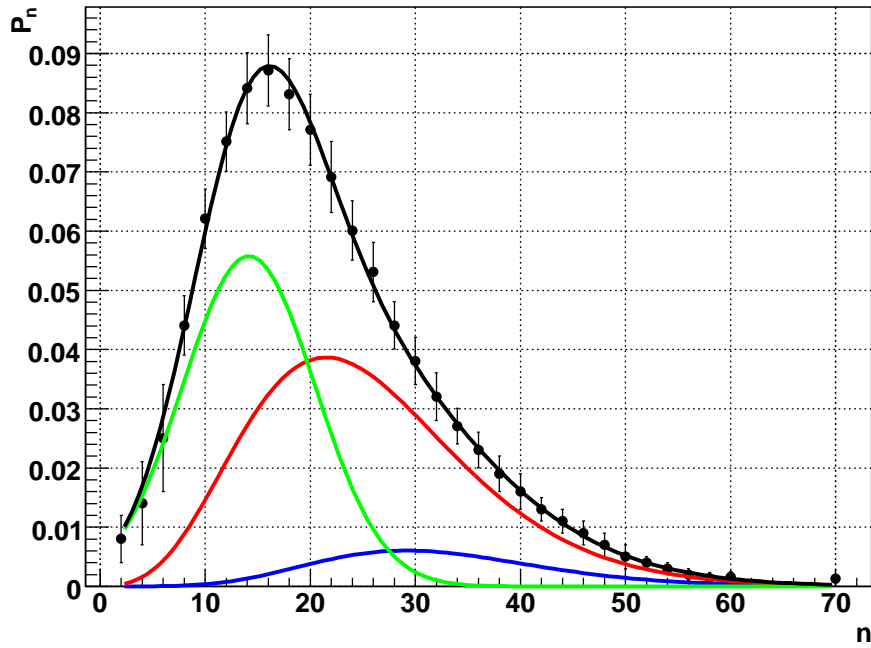


Figure 11: Charged multiplicity distribution for proton-antiproton scattering, $\sqrt{s} = 200$ GeV [10]. Blue line – negative binomial distribution for three quark strings, red line – negative binomial distribution for two quark strings, green line – Gaussian distribution for gluon string, black line is sum of these distributions, $\chi^2/ndf = 4/26$.

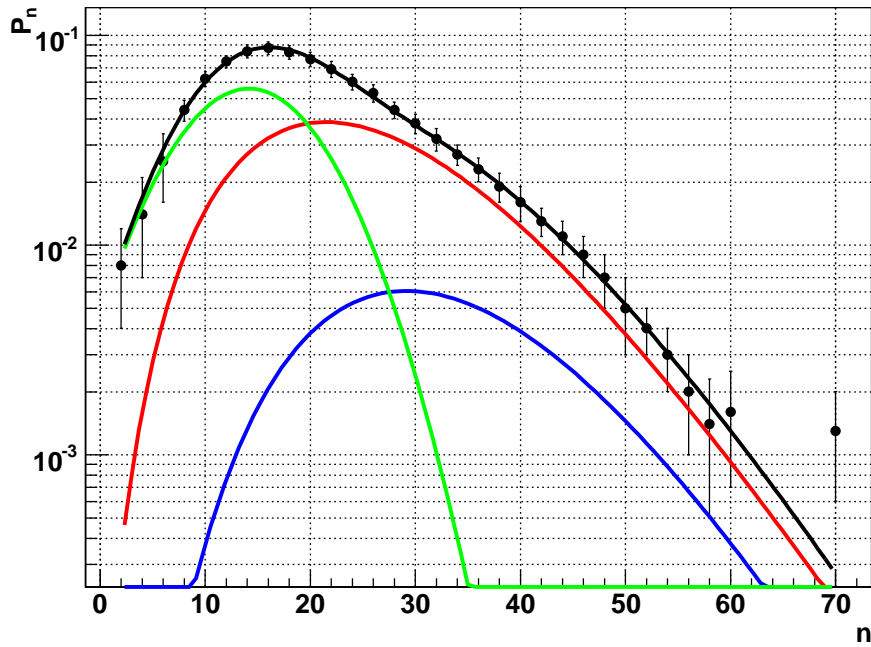


Figure 12: The same as for Fig. 11, logarithmic scale.

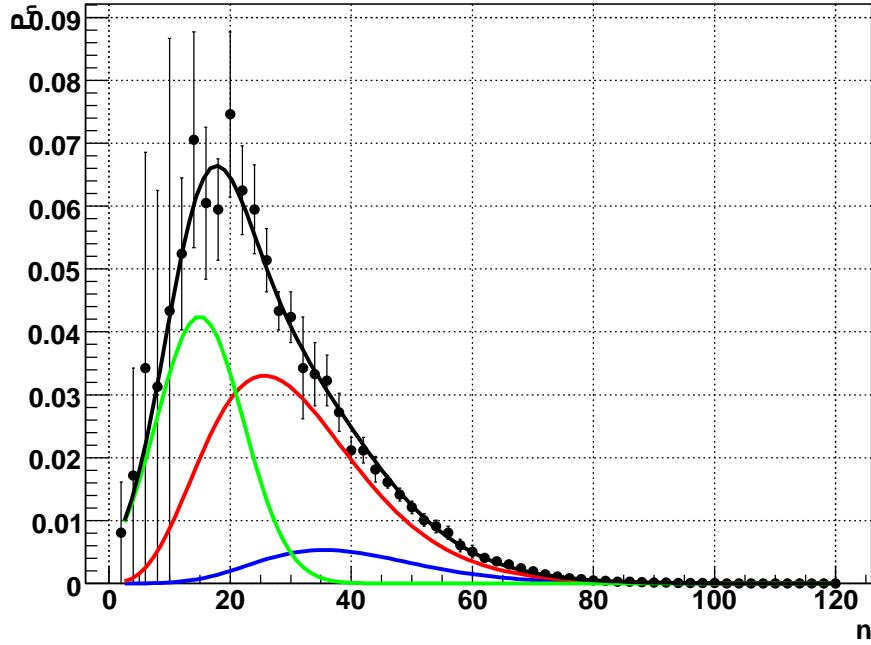


Figure 13: Charged multiplicity distribution for proton-antiproton scattering, $\sqrt{s} = 300$ GeV [11]. Blue line – negative binomial distribution for three quark strings, red line – negative binomial distribution for two quark strings, green line – Gaussian distribution for gluon string, black line is sum of these distributions, $\chi^2/ndf = 19/55$.

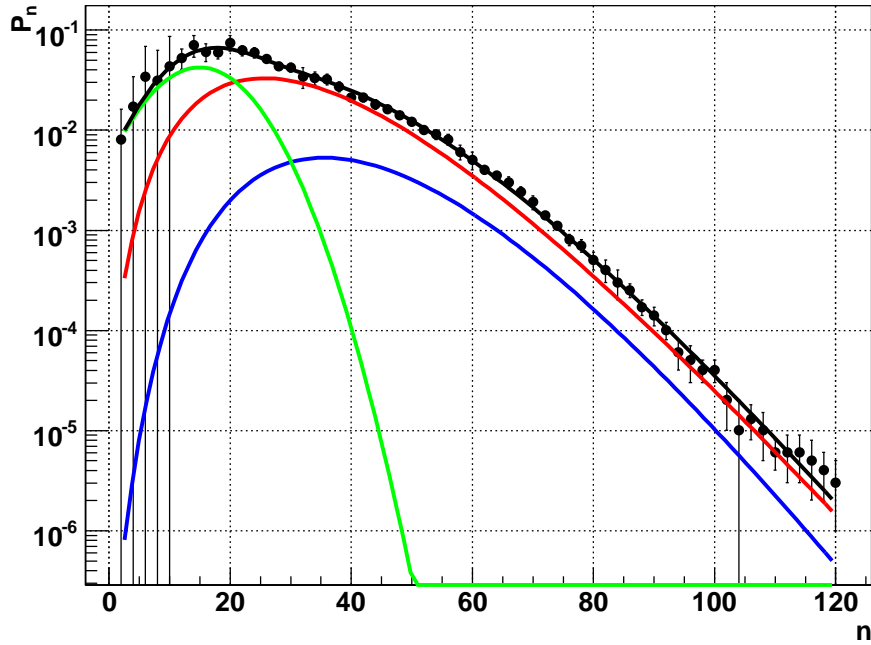


Figure 14: The same as for Fig. 13, logarithmic scale.

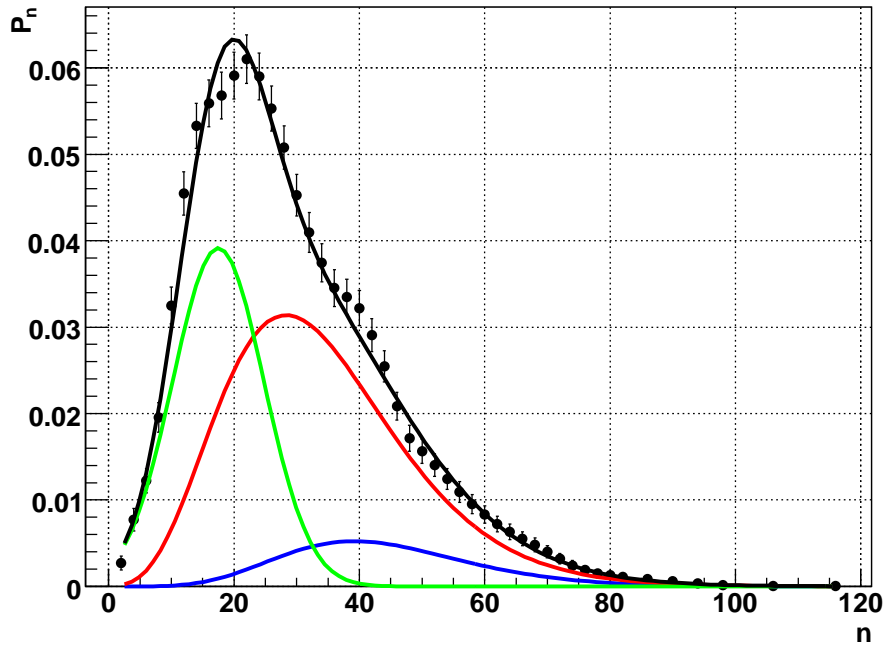


Figure 15: Charged multiplicity distribution for proton-antiproton scattering, $\sqrt{s} = 546$ GeV [6]. Blue line – negative binomial distribution for three quark strings, red line – negative binomial distribution for two quark strings, green line – Gaussian distribution for gluon string, black line is sum of these distributions, $\chi^2/ndf = 36/42$.

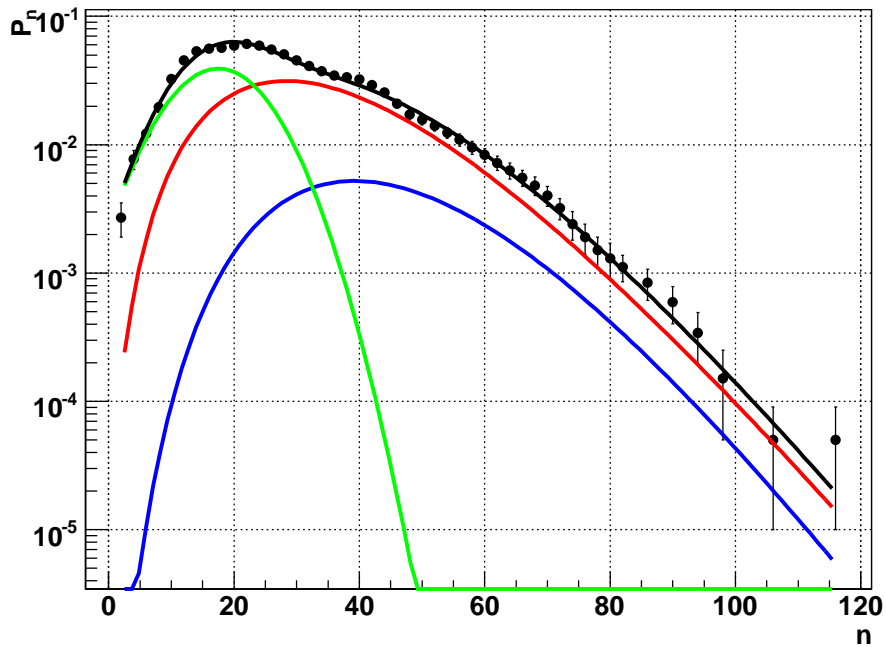


Figure 16: The same as for Fig. 15, logarithmic scale.

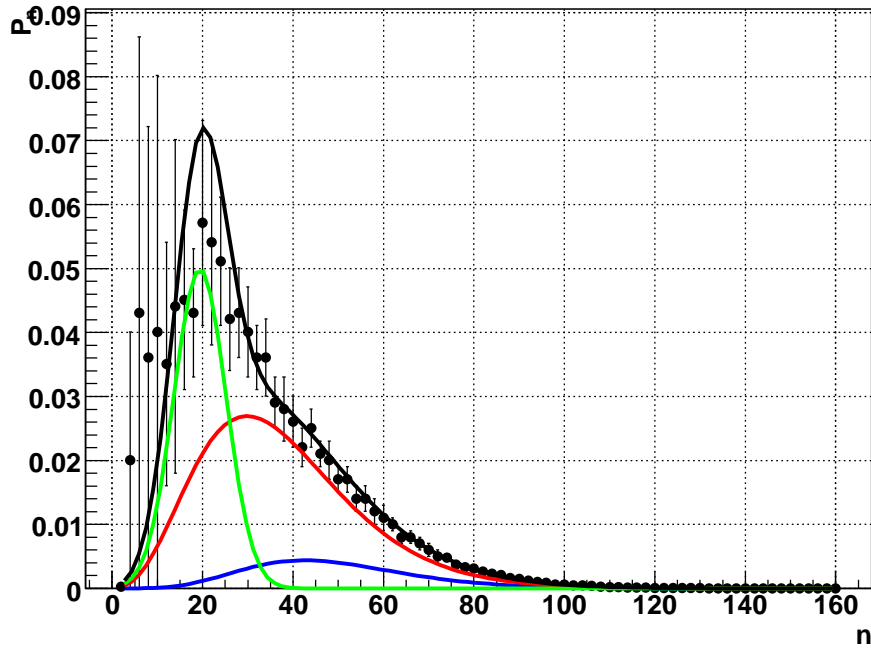


Figure 17: Charged multiplicity distribution for proton-antiproton scattering, $\sqrt{s} = 546$ GeV [11]. Blue line – negative binomial distribution for three quark strings, red line – negative binomial distribution for two quark strings, green line – Gaussian distribution for gluon string, black line is sum of these distributions, $\chi^2/ndf = 33/76$.

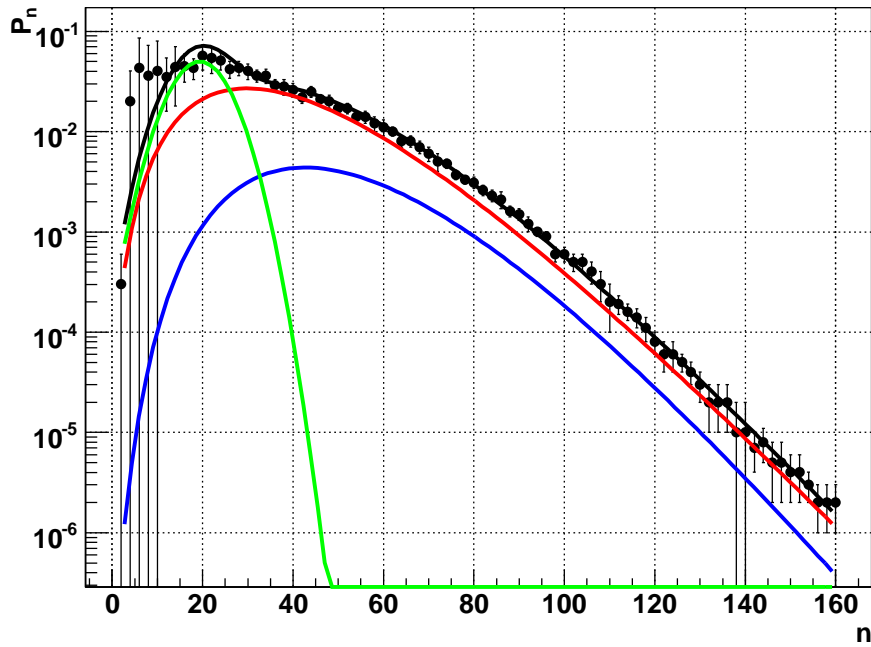


Figure 18: The same as for Fig. 17, logarithmic scale.

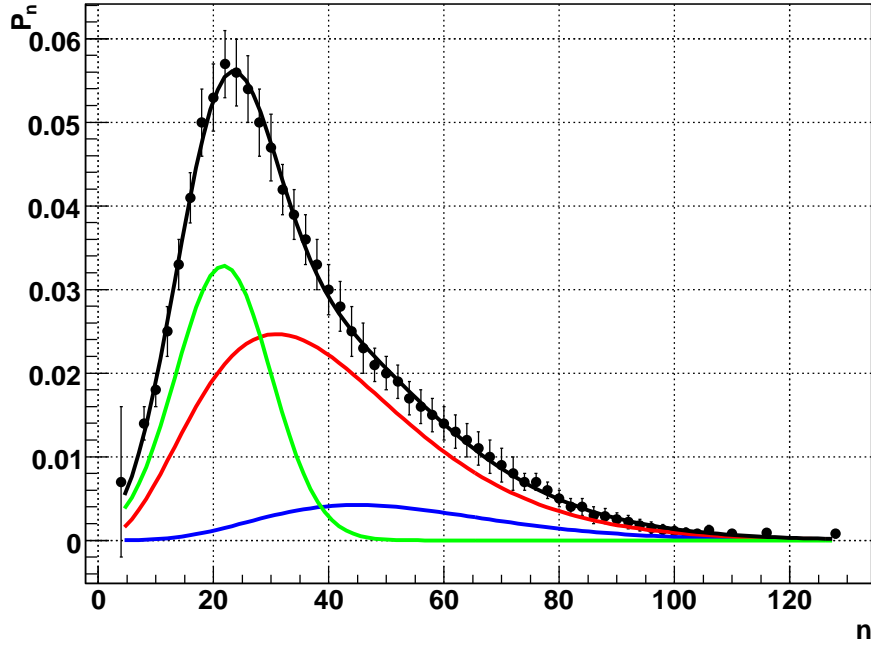


Figure 19: Charged multiplicity distribution for proton-antiproton scattering, $\sqrt{s} = 900$ GeV [10]. Blue line – negative binomial distribution for three quark strings, red line – negative binomial distribution for two quark strings, green line – Gaussian distribution for gluon string, black line is sum of these distributions, $\chi^2/ndf = 8/49$.

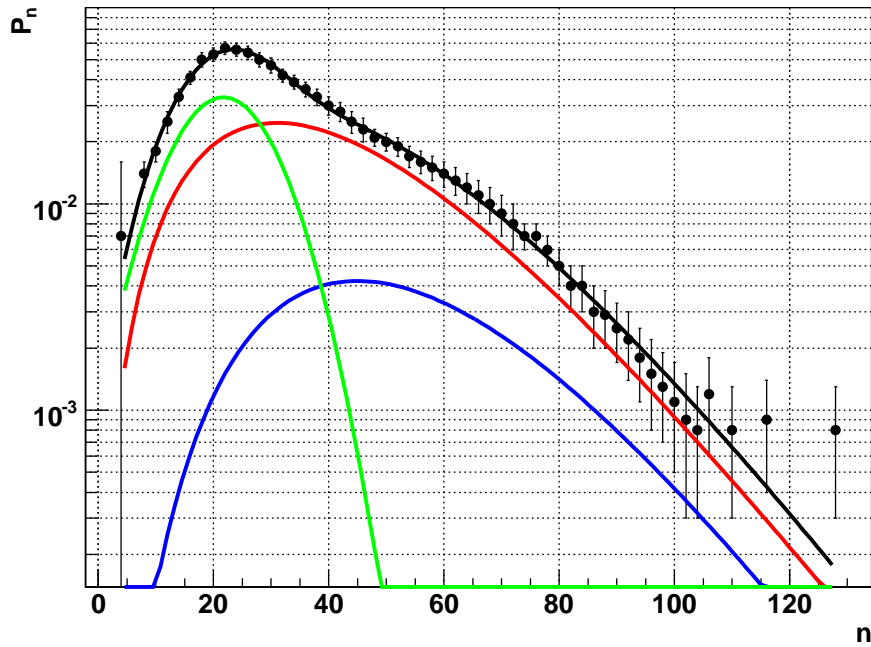


Figure 20: The same as for Fig. 19, logarithmic scale.

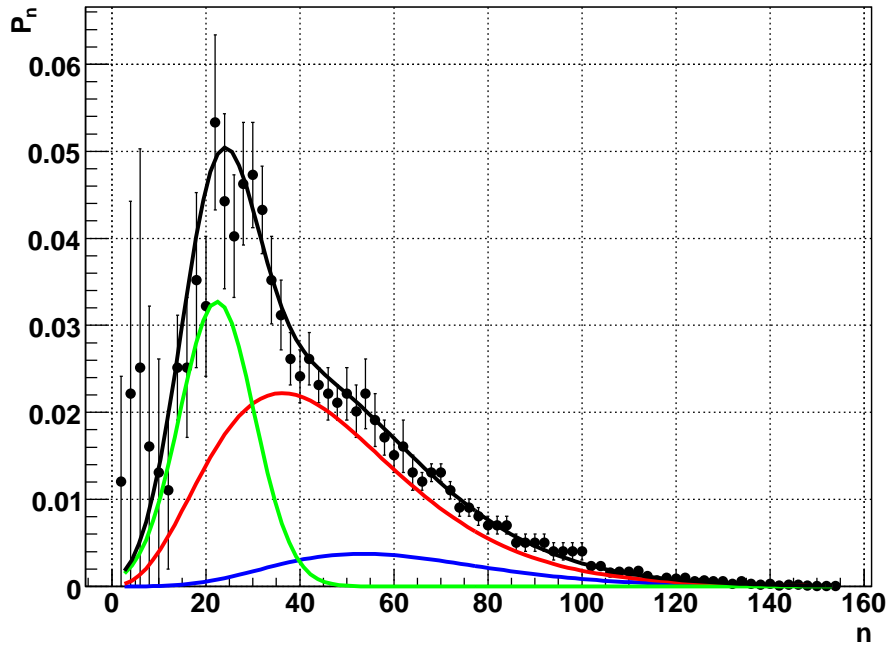


Figure 21: Charged multiplicity distribution for proton-antiproton scattering, $\sqrt{s} = 1000$ GeV [11]. Blue line – negative binomial distribution for three quark strings, red line – negative binomial distribution for two quark strings, green line – Gaussian distribution for gluon string, black line is sum of these distributions, $\chi^2/ndf = 53/73$.

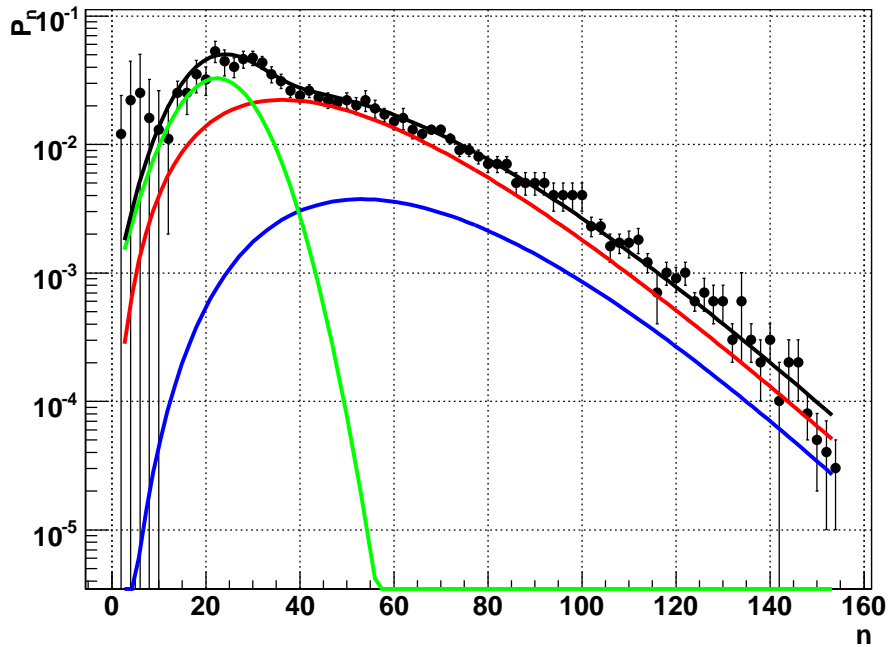


Figure 22: The same as for Fig. 21, logarithmic scale.

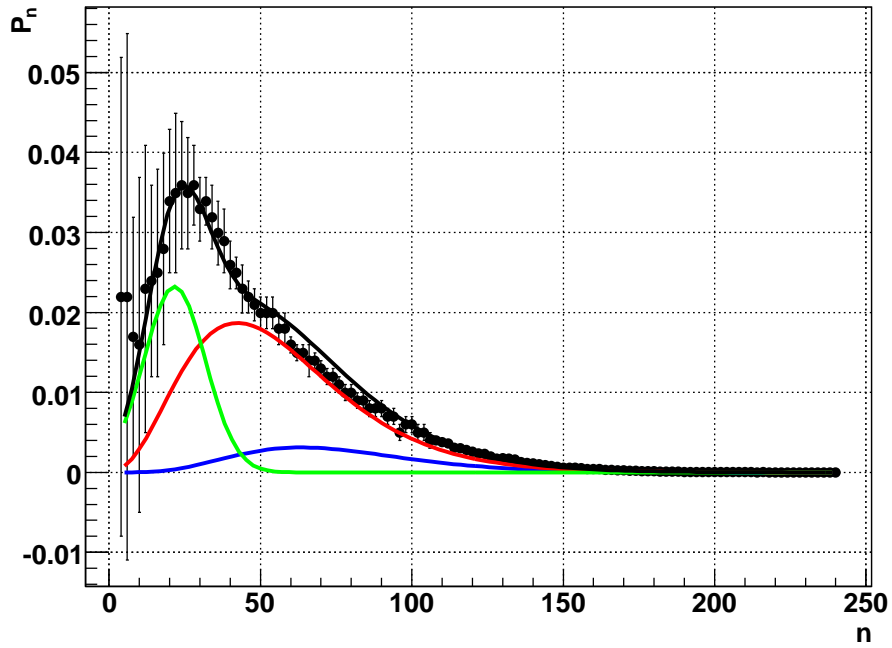


Figure 23: Charged multiplicity distribution for proton-antiproton scattering, $\sqrt{s} = 1800$ GeV [11]. Blue line – negative binomial distribution for three quark strings, red line – negative binomial distribution for two quark strings, green line – Gaussian distribution for gluon string, black line is sum of these distributions, $\chi^2/ndf = 120/115$.

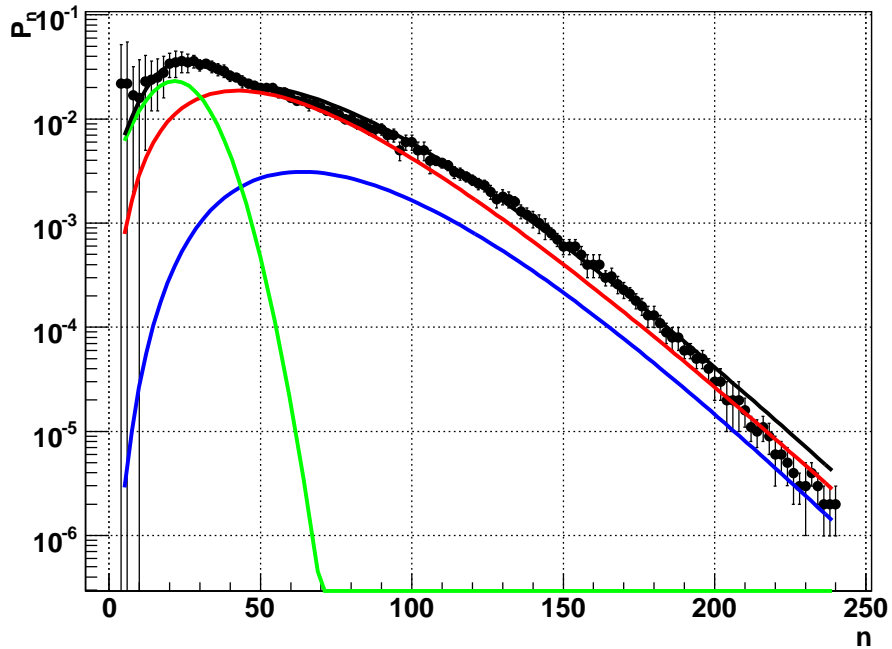


Figure 24: The same as for Fig. 23, logarithmic scale.

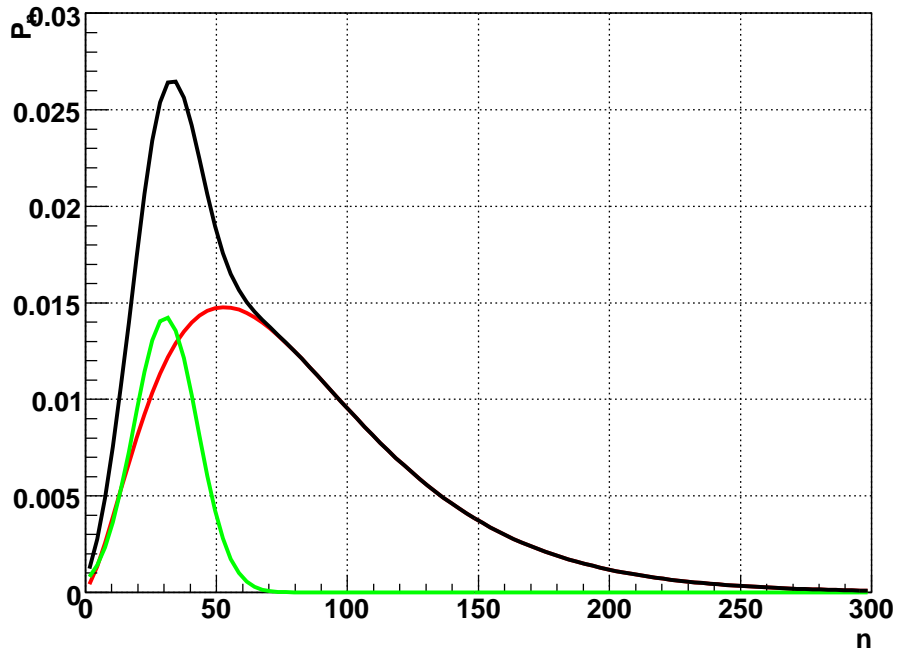


Figure 25: Charged multiplicity distribution for proton-antiproton scattering, $\sqrt{s} = 14$ TeV. Red line – negative binomial distribution for two quark strings, green line – Gaussian distribution for gluon string, black line is sum of these distributions.

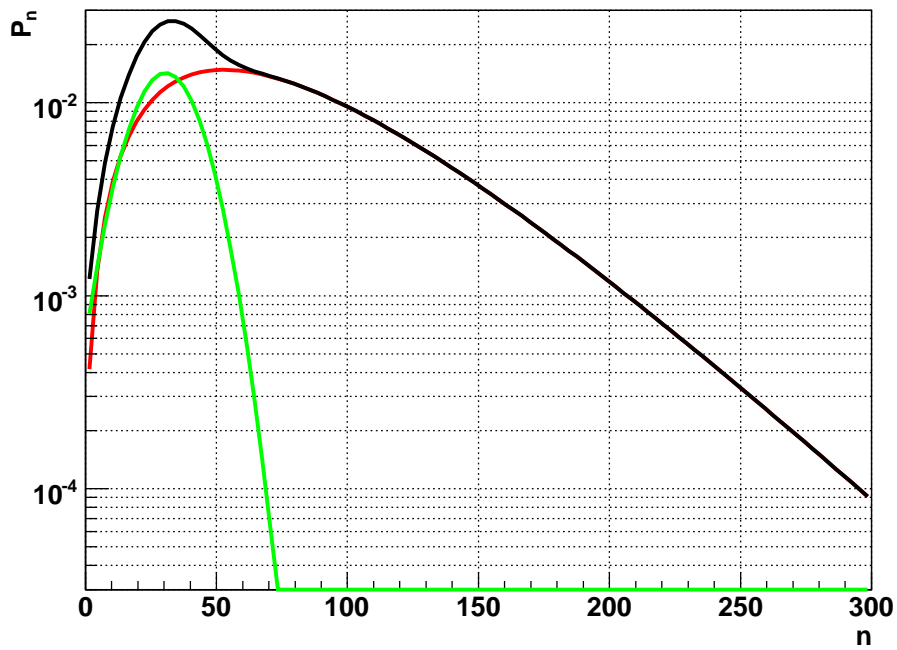


Figure 26: The same as for Fig. 25, logarithmic scale.

5 Conclusion

The main results of this work are the following: we have calculated the charged multiplicity distribution and its mean value $\langle n \rangle = 71.57 \pm 4.37$, and total cross section $\sigma_{tot}^{pp} = 101.30 \pm 6.65$ mb for energy $\sqrt{s} = 14$ TeV.

It was shown that multiplicity distributions are determined by contributions of inelastic processes of new type. These inelastic processes completely differ from inelastic processes originating from unitary cuts of pomeron and pomeron branchings [12], [13]. These are processes of hadrons production in gluon string and in two quark strings for proton-proton scattering and processes of hadrons production in gluon string and in two and three quark strings for proton-antiproton scattering.

It is necessary to emphasize that inelastic processes for proton-proton scattering differ from inelastic processes for proton-antiproton scattering.

We are grateful to O.V. Kancheli for useful discussions.

References

- [1] E.A. Kuraev, L.N. Lipatov, V.S. Fadin, Zh.Eksp.Teor.Fiz. **72**, 377 (1977).
- [2] V.A. Abramovsky, O.V. Kancheli, Pisma Zh.Eksp.Teor.Fiz. **32**, 498 (1980).
- [3] V.A. Abramovsky, O.V. Kancheli, Pisma Zh.Eksp.Teor.Fiz. **31**, 566 (1980).
- [4] C. Amsler et al., Review of Particle Physics, Phys. Lett. B. **667**, 1 (2008).
- [5] G.J. Alner et al. (UA5 Collaboration), ZP **C32**, 153 (1986).
- [6] G.J. Alner et al. (UA5 Collaboration), Phys. Rep. **154**, 247 (1987).
- [7] F. Abe et al. (CDF Collaboration), Phys. Rev. **D50**, 5550 (1994).
- [8] N.A. Amos et al. (E710 Collaboration), Phys. Lett. **B243**, 158 (1990).
- [9] A. Breakstone et al. (ABCDHW Collaboration), Phys. Rev. **D30**, 528 (1984).
- [10] R.E. Ansorge et al. (UA5 Collaboration), ZP **C43**, 357 (1989).
- [11] T. Alexopoulos et al. (E735 Collaboration), Phys. Lett. **B435**, 453 (1998).
- [12] V.A. Abramovsky, O.V. Kancheli, Pisma Zh.Eksp.Teor.Fiz. **15**, 559 (1972).
- [13] V.A. Abramovsky, V.N. Gribov, O.V. Kancheli, Yad.Fiz. **18**, 413 (1973).